
ELSEVIER
QUATERNARY
SCIENCE REVIEWS
The International Multidisciplinary Research and Review Journal

Quaternary Science Reviews 55 (2012) 50–58

Contents lists available at SciVerse ScienceDirect

Quaternary Science Reviews

journal homepage: www.elsevier.com/locate/quascirev

Holocene palaeoenvironmental history of the Amazonian mangrove belt

Marcelo Cancela Lisboa Cohen[a,b,*], Luiz Carlos Ruiz Pessenda[c], Hermann Behling[d], Dilce de Fátima Rossetti[e], Marlon Carlos França[a], José Tasso Felix Guimarães[a], Yuri Friaes[a], Clarisse Beltrão Smith[a]

[a] Laboratory of Coastal Dynamics, Programa de Pós-Graduação em Geologia e Geoquímica, Instituto de Geociências, Universidade Federal do Pará (UFPA), Rua Augusto Correa 01, 66075-110 Belém, PA, Brazil
[b] Oceanography Faculty, Federal University of Pará, Rua Augusto Corrêa, n 1, Guama, 66075-110 Belém, PA, Brazil
[c] Centro de Energia Nuclear na Agricultura (CENA), 13400-000 Piracicaba, SP, Brazil
[d] Department of Palynology and Climate Dynamics, Albrecht-von-Haller-Institute for Plant Sciences, University of Göttingen, Untere Karspüle 2, 37073 Göttingen, Germany
[e] National Space Research Institute (INPE), Rua dos Astronautas 1758-CP 515, 12245-970 São José dos Campos, SP, Brazil

ARTICLE INFO

Article history:
Received 20 April 2012
Received in revised form
27 August 2012
Accepted 29 August 2012
Available online

Keywords:
Carbon and nitrogen isotopes
C/N
Climatic changes
Northern Amazonia
Palynology
Sea-level

ABSTRACT

Wetland dynamic in the northern Brazilian Amazon region during the Holocene was reviewed using palynological, carbon and nitrogen isotopes records, and C/N ratio previously published. The integration of 72 radiocarbon dates recorded in 34 sediment cores sampled along the marine and fluvial littoral, and mainly influenced by the Amazon River, reveals that marine influence and mangrove vegetation were wider than today on the mouth of Amazon River between >8990–8690 and 2300–2230 cal yr BP, forming a continuous mangrove belt along the northern Brazilian Amazon littoral. The establishment of this mangrove strip is a direct consequence of the marine incursion caused by post-glacial sea-level rise possibly associated with tectonic subsidence during the Early and Middle Holocene. In the Late Holocene, in areas influenced by the Amazon River discharge, the mangroves were replaced by freshwater vegetation, and the coast morphology evolved from an estuarine dominated into a rectilinear coast due to coastal progradation. Nevertheless, the marine-influenced littoral, which is currently dominated by mangroves and salt-marsh vegetation, has persistently had brackish water vegetation over tidal mud flats throughout the entire Holocene. Likely, the fragmentation of this continuous mangrove line during the Late Holocene was caused by the increase of river freshwater discharge associated to the change from dry into wet climates in the Late Holocene. This caused a significant decrease of tidal water salinity in areas near the mouth of Amazon River. These changes in the Amazon discharge are probably associated with dry and wet periods in the northern Amazon region during the Holocene.

1. Introduction

Global mangrove distributions have fluctuated throughout geological and human history. The area covered by mangroves is influenced by a complex interaction involving gradients of tidal inundation frequency, waterlogging, nutrient availability and soil salt concentration across the intertidal area (Hutchings and Saenger, 1987; Wolanski et al., 1990). The geomorphic setting of mangrove systems also comprises a range of inter-related factors such as substrate types, coastal processes, sediment and freshwater delivery. All of these influence the occurrence and survivorship of mangroves (Semeniuk, 1994).

Approximately 85% of Brazilian mangroves occur along 1800 km of the northern coast in the states of Amapá, Pará and Maranhão, which together contain 10,713 km^2 of these ecosystems (Schaeffer-Novelli et al., 1990; Vannucci, 1999), and hold one of the world's largest mangrove areas (Kjerfve and Lacerda, 1993). The continuity of this mangrove littoral is interrupted by the area influenced by the Amazon River water discharge, where *várzea* (seasonally flooded) vegetation dominates (Cohen et al., 2008). Thus, climatic and hydrological factors have mainly controlled the geobotanical units of the Amazon coast leading to the formation of: 1) a marine-influenced littoral, submitted to tidal water salinity between 30‰ and 7‰ (southeastern and northwestern coastline) and dominated by mangroves and salt-marsh vegetation; and 2) a fluvial sector, close to the Amazon River mouth, with tidal water salinity below

* Corresponding author. Oceanography Faculty, Federal University of Pará, Rua Augusto Corrêa, n 1, Guama, 66075-110 Belém, PA, Brazil. Tel./fax: +55 91 3274 3069.
E-mail address: mcohen@ufpa.br (M.C.L. Cohen).

0277-3791/$ – see front matter © 2012 Elsevier Ltd. All rights reserved.
http://dx.doi.org/10.1016/j.quascirev.2012.08.019

7‰ (Monteiro, 2009), characterized by *várzea* and herbaceous vegetation (Cohen et al., 2009).

The Holocene vegetation history along the littoral of northern Brazil was characterized by mangrove establishment and expansion/contraction phases (Behling, 1996, 2001; Behling et al., 2001; Cohen et al., 2005a,b, 2008, 2009; Vedel et al., 2006; Smith et al., 2011; Guimarães et al., 2012). These phases have been related to changes in relative sea-level and/or river water discharge, since the current distribution of mangrove on this littoral is mainly controlled by substratum topography and freshwater discharge (Cohen et al., 2005a,b; Lara and Cohen, 2006, 2009).

Rainfall variations in the Amazonian hydrographic region (Van der Hammen, 1974; Absy et al., 1991; Desjardins et al., 1996; Behling and Costa, 2000; Ledru, 2001; Pessenda et al., 2001) likely control the volume of the Amazon River, which displays the world's greatest water discharge of 6300 $km^3\ yr^{-1}$ (Eisma et al., 1991; Maslin and Burns, 2000; Latrubesse and Franzinelli, 2002). Consequently, during the drier chronologies of the Early and Middle Holocene, the Amazon River's inflow may have been severely reduced (Amarasekera et al., 1997; Toledo and Bush, 2007, 2008). Thus, significant changes in river water discharge along the littoral would be expected and would have affected salinity gradients along the coastline influenced by the Amazon River. Therefore, this process could have affected the distribution of mangrove (brackish water vegetation) and *várzea*/herbaceous vegetation (freshwater vegetation) in the Northern Brazilian littoral.

In this framework, and based on the integration of previously published studies such as pollen, $\delta^{13}C$, $\delta^{15}N$ and C/N analyses chronologically contextualized with radiocarbon data, this paper proposes to characterize changes in the northern Amazonian mangrove belt during the Holocene according to post-glacial sea-level rise and dry and wet periods recorded in the region.

2. Study area

The study sites are located in northern Brazil, along the Pará and Amapá littoral (Fig. 1). Calçoene, Amapá (Guimarães et al., 2012), Salinópolis, São Caetano, Soure and Bragança mangroves (Behling et al., 2001, 2004; Cohen et al., 2005a,b, 2009; Vedel et al., 2006; França et al., in press) are part of the wetland system influenced by tidal water salinity between 30‰ and 7‰. This coastal mangrove belt is interrupted by a *várzea* vegetation area under the Amazon River influence (Cohen et al., 2008). Lake Arari (Smith et al., 2011, 2012) and the town of Macapá (Guimarães et al., 2012) are located under such conditions.

The climate is a warm and humid tropical one, with a mean annual temperature of 27 °C and mean annual precipitation of approximately 3000 mm, concentrated between January and June (IDESP, 1974). The mean Amazon River discharge is about 170,000 $m^3\ s^{-1}$ (at Óbidos city), with maximum and minimum outflow of 270,000 and 60,000 $m^3\ s^{-1}$ (ANA, 2003). The Amazon estuary is classified as semidiurnal macrotidal (Pugh, 1987), with a tidal range of 4–6 m (Gallo and Vinzon, 2005). The structure of the plume is controlled by the North Brazilian Current, which induces a northwestern flow with speeds of 40–80 cm/s over the continental shelf (Fig. 1) (Lentz and Limeburner, 1995), strong

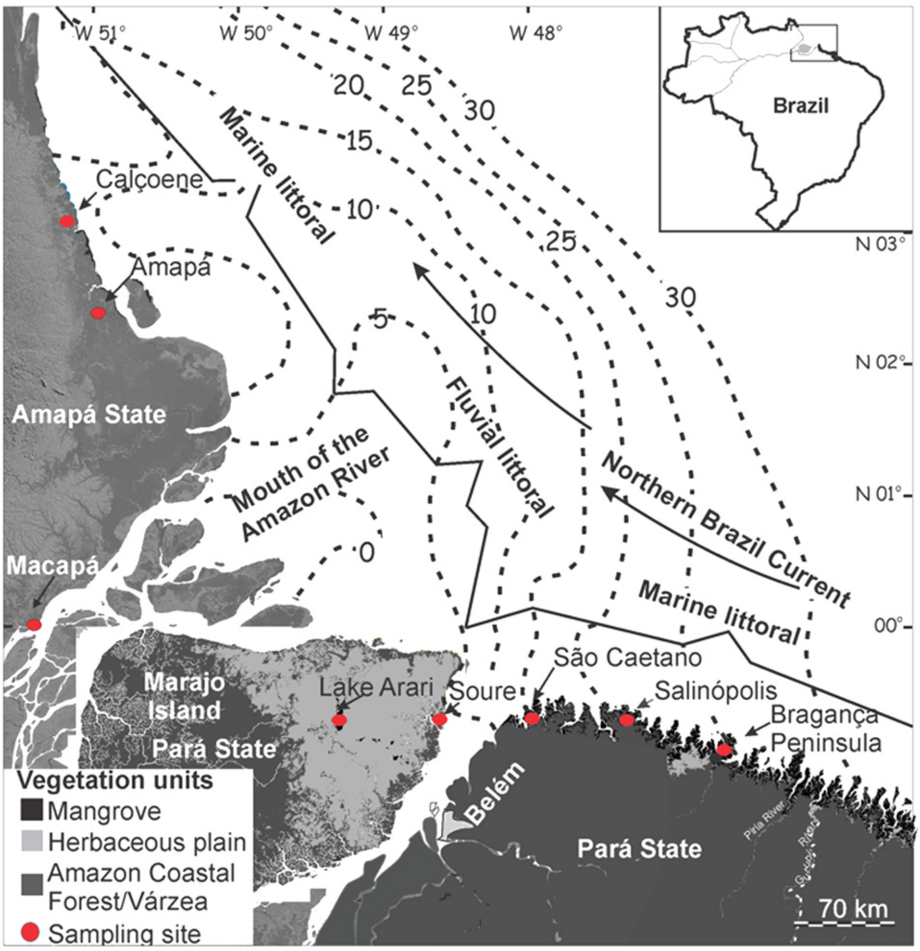

Fig. 1. Location of the study areas and the sea water salinity, Amazon River plume and North Brazil Current.

tidal currents (Beardsley et al., 1995) and trade winds (Lentz and Limeburner, 1995). Consequently, the river discharge and hydrodynamic conditions allow a strong reduction of water salinity along the Amazon River and adjacent coast (Fig. 1) (Vinzon et al., 2008; Rosario et al., 2009).

The marine influenced littoral is characterized by peninsulas crossed by tidal channels that link wetlands with the estuaries, in particular of the eastern coastal region of Pará State. The main hydrodynamic features are macrotides of ∼4 m range and current velocities reaching ∼1.5 m s^{-1} for spring tides (Cohen et al., 1999). The modern vegetation is represented by the following units: Amazon coastal forest (composed of terrestrial trees such as *Coccoloba latifolia*, *Himatanthus articulata*, *Anacardium occidentale*, *Protium heptaphyllum*, *Ouratea castanaefolia*, *Ouratea microdonta*, *Tapirira guianensis*, *Myrcia fallax*, *Myrcia sylvatica*, *Eugenia patrisi*, *Cedrela odorata*, *Hymenaea courbaril* and *Manilkara huberi*), elevated herbaceous flats (e.g., *Eleocharis geniculata*, *Fimbristylis spadicea*, *Sporobolus virginicus*, *Sesuvium portulacastrum*), mangroves (*Rhizophora mangle*, *Avicennia germinans*, *Laguncularia racemosa*), and *restinga* (*Chrysobalanus icaco*, *Anacardium occidentale*, *Byrsonima crassifolia*) (Cohen et al., 2005a, 2009).

The fluvial littoral is represented by part of the Amapá State and the Marajó Island. The vegetation consists of natural open areas dominated by Cyperaceae and Poaceae that widely colonize the eastern side of the Marajó island. The *várzea* vegetation (a seasonally inundated floodplain and a swamp permanently inundated by freshwater, composed of wetland species such as the palm trees *Mauritia flexuosa* and *Euterpe oleracea*, and other species such as *Hevea guianensis* (Zarin et al., 2001; Junk and Piedade, 2004; McGinley, 2007)) and Amazon Coastal Forest occur on the western side of the island (Cohen et al., 2008). Mangroves are restricted to a small area (100–700 m in width) along the northeastern coastal plain of the Marajó Island (França et al., in press).

3. Materials and methods

3.1. Sampling

In total 10 sediment cores were sampled from fluvial influenced littoral in the Marajó Island and Macapá coastline. Twenty-four cores were sampled along the marine littoral; the cores were situated in the northwestern Amapá, Salinópolis, São Caetano, Soure and Bragança littoral (Table 1). The product of integration of these 34 cores is represented in the 17 sediment cores that are the longest chronologically. The other sediment cores that were chronologically shortest confirm the trends presented in Fig. 2.

3.2. Palynological analysis

Cores were sub-sampled at intervals of 5 cm and 1 cm^3 of sediment was taken for palynological analysis. Samples were prepared using standard techniques for the extraction of palynomorphs, including acetolysis (Faegri and Iversen, 1989). Handbooks of pollen and spores morphology were consulted (Roubik and Moreno, 1991; Colinvaux et al., 1999; Hesse et al., 2008) as

Table 1
Sediment cores with their respective locations, marine or fluvial influence, amount of dates, type of analysis (P, palynology; I, isotope), depth and reference.

Core	Location	Sampling site	Influence	Number of dates	Analysis type	Depth (cm)	Reference
R-1	S00°40′26.3″/ W048°29′37.2″	Soure	Marine	1	P/I	150	França et al. (in press)
R-2	S00°40′23.1″/ W048°29′38.8″	Soure	Marine	1	P/I	150	França et al. (in press)
R-3	S0°40′25.2″/W48°29′35.7″	Soure	Marine	2	P/I	150	França et al. (in press)
R-4	S00°39′37″/W048°29′3.3″	Soure	Marine	6	P/I	220	França et al. (in press)
R-5	S00°55′41″/W048°39′47″	Arari/Soure	Fluvial	5	P/I	251	França et al. (in press)
BV	S0°43′10″/W48°29′32″	Soure	Marine	4	P	140	Behling et al. (2004)
PP	S0°39′34.0″/W48°29′00″	Soure	Marine	3	P	120	Behling et al. (2004)
LA-A	S00°35′52″/W49°08′35″	L.Arari	Fluvial	1	P/I	62	Smith et al. (2011)
LA-B	S00°35′54″/W49°09′49″	L.Arari	Fluvial	2	P/I	82	Smith et al. (2011)
LA-C	S00°39′39″/W49°09′20″	L.Arari	Fluvial	1	P/I	50	Smith et al. (2012)
LA-D	S00°43′40″/W49°10′00″	L.Arari	Fluvial	3	P/I	80	Smith et al. (2012)
LA-E	S00°43′24″/W49°09′41″	L.Arari	Fluvial	2	P	150	Cohen et al. (2008)
HP-A	S00°53′34″/W48°40′8″	L.Arari	Fluvial	1	P	32	Smith et al. (2011)
S1	S01°00′26″/W48°56′18″	L.Arari	Fluvial	1	P	45	Cohen et al. (2008)
S2	S00°56′41″/W48°42′44″	L.Arari	Fluvial	1	P	28	Cohen et al. (2008)
MAC	N00°04′15″/W51°02′15″	Macapá	Fluvial	3	P/I	200	Guimarães et al. (2012)
AM	N02°03′08″/W50°48′21″	Amapá	Marine	2	P/I	100	Guimarães et al. (2012)
GV	N02°34′38″/W50°53′17″	Calçoene	Marine	1	P/I	70	Guimarães et al. (2012)
GA	N02°35′59″/W50°52′08″	Calçoene	Marine	1	P/I	127	Guimarães et al. (2012)
GP	N02°36′48″/W50°50′41″	Calçoene	Marine	1	P/I	137	Guimarães et al. (2012)
M1	S0°53′24″/W46°40′24″	Bragança	Marine	1	P	10	Cohen et al. (2005a)
M3	S0°53′53″/W46°40′27″	Bragança	Marine	1	P	30	Cohen et al. (2005a)
M2	S0°53′53″/W46°40′27″	Bragança	Marine	1	P	27.5	Cohen et al. (2005a)
M9	S0°54′03.9″/W46°40′40″	Bragança	Marine	1	P	32	Cohen et al. (2005a)
M5	S0°54′15.2″/W46°40′59″	Bragança	Marine	2	P	57	Cohen et al. (2005a)
RKS3	S0°51′48″/W46°39′04″	Bragança	Marine	1	P	351	Cohen et al. (2005b)
M6	S00°54′28″/W46°41′25″	Bragança	Marine	1	P	57.5	Cohen et al. (2005a)
CS	S05°40′46″/W46°40′63″	Bragança	Marine	3	P	135	Cohen et al. (2005b)
BA	S05°50′65″/W46°40′00″	Bragança	Marine	3	P	540	Cohen et al. (2005b)
FC	S00°52′25″/W46°39′00″	Bragança	Marine	3	P	179	Cohen et al. (2005b)
TAP	S00°58′18″/W46°47′24″	Bragança	Marine	6	P	385	Vedel et al. (2006)
APL	S00°36′/W47°17′	Salinópolis	Marine	2	P	40	Cohen et al. (2009)
AB	S00°38′/W47°18′	Salinópolis	Marine	2	P	230	Cohen et al. (2009)
SC	S00°43′/W48°01′	S. Caetano	Marine	3	P	600	Cohen et al. (2009)

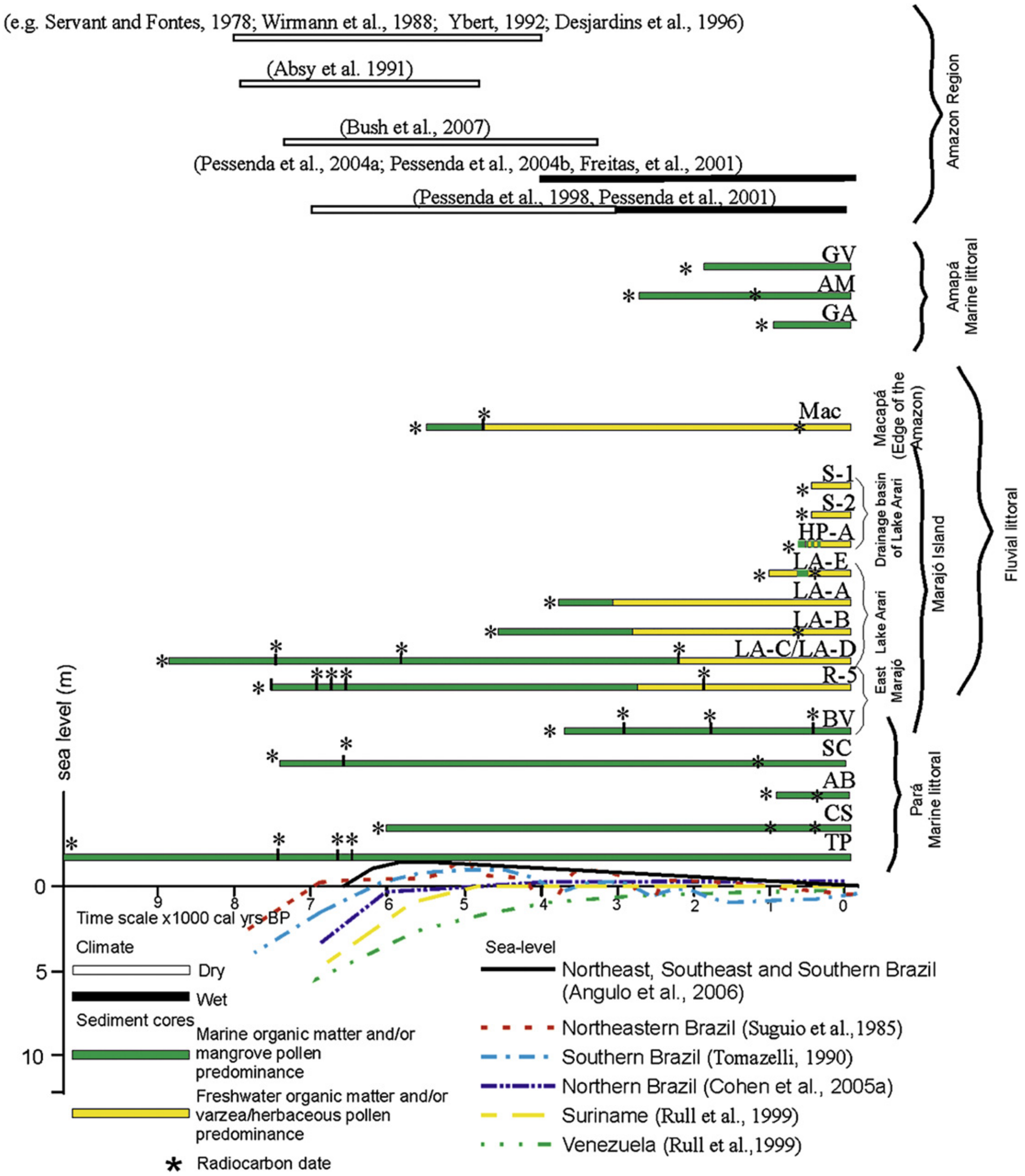

Fig. 2. Comparative diagram of climatic change records in the Amazon region, sea-level rise in eastern South America during the Holocene and pollen diagrams from the littoral of Pará and Amapá.

well as the reference collections of the "Laboratório de Dinâmica Costeira – UFPa" and of Hermann Behling to identify pollen grains and spores. A minimum of 300 pollen grains were counted per sample.

3.3. C/N, carbon and nitrogen isotopes

The $\delta^{13}C$, $\delta^{15}N$ and elemental C and N (C/N) concentrations were analyzed from samples (6–50 mg) taken at 5 cm intervals along the cores sampled from Amapá and Marajó Island. The stable carbon and nitrogen isotopes as well as the total organic carbon (TOC) and nitrogen (TN) were determined at the Stable Isotopes Laboratory at the Center for Nuclear Energy in Agriculture (CENA), University of Sao Paulo (USP), using a Continuous Flow Isotopic Ratio Mass Spectrometer (CF-IRMS). Further details may be found in Smith et al. (2012).

3.4. Radiocarbon dating

Seventy-two bulk samples of ~2 g each were used for radiocarbon dating (Table 2). Samples were checked and physically cleaned under the microscope. The residual material was then extracted with 2% HCl at 60 °C over 4 h, washed with distilled water until pH was neutral and dried (50 °C). The sediment organic matter was analyzed by Accelerator Mass Spectrometry (AMS) at the Center for Applied Isotope Studies (Athens, Georgia, USA), at the Leibniz Laboratory of Isotopic Research at Christian-Albrechts University in Kiel (Germany), at the Physic Institute at the University of Erlangen (Germany), and at the Van der Graaff Laboratory at the Utrecht University (The Netherlands). Radiocarbon ages are reported in years before AD 1950 (yr BP) normalized to $\delta^{13}C$ of -25‰VPDB and in cal yr BP with a precision of 2σ (Reimer et al., 2009).

Table 2
Radiocarbon ages (AMS). Radiocarbon ages are presented in conventional yr BP and in cal yr BP (±2σ), obtained with software package Calib 6.0 and the Intcal09 curve (Reimer et al., 2009). UGAMS – AMS Laboratory at the University of Georgia-USA, KIA – Leibniz Laboratory of Isotopic Research at the University in Kiel (Germany), ERL – Physic Institute at the University of Erlangen (Germany) and UTC – Van der Graaff Laboratory at the Utrecht University (Netherland).

Sample	Lab. Number	Depth (cm)	Cal yr BP
R-1	UGAMS4924	147–150	560–520
R-2	UGAMS4925	147–150	1160–1120
R-3	UGAMS4927	107–110	70–30
R-3	UGAMS4926	147–150	680–640
R-4	UGAMS4931	3	Modern
R-4	UGAMS5316	44–46	Modern
R-4	UGAMS5317	65–69	614–552
R-4	UGAMS4932	190–192	1518–1453
R-4	UGAMS5318	209–211	1419–1334
R-4	UGAMS4933	218–220	1739–1567
R-5	UGAMS4928	22–24	1947–1813
R-5	UGAMS8209	78–83	6633–6579
R-5	UGAMS4929	142–146	6737–6597
R-5	UGAMS8208	234–240	6772–6768
R-5	UGAMS4930	248–251	7521–7433
BV20	KIA19811	20	Modern
BV40	KIA19812	40	537–493
BV100	KIA19813	100	1843–1793
BV140	KIA19404	140	4023–3933
PP20	KIA19809	20	Modern
PP60	KIA19810	60	Modern
PP120	KIA19402	120	647–597
LA-A	KIA34340	62	3795–3706
LA-B	KIA34341	33	670–632
LA-B	KIA34342	82	4530–4423
LA-C	KIA34343	50	8990–8691
LA-D	UGAMS6999	20	2306–2234
LA-D	KIA34344	30	5944–5888
LA-D	KIA34345	80	7328–7168
LA-E	KIA28165	100	592–542
LA-E	KIA28166	150	1228–1164
HP-A	KIA28165	32	660–626
S1	KIA28167	45	564–504
S2	KIA28168	28	562–512
MAC 20	UGAMS5311	20	600–560
MAC 145	UGAMS5312	145	5290–5150
MAC 200	UGAMS5313	200	5560–5470
AM 60	UGAMS5314	60	1260–1080
AM 100	UGAMS5315	100	2350–2300
GV	KIA28169	70	2160–2040
GA	KIA28170	127	1005–935
GP	KIA28171	137	3630–3350
M1/10 cm	KIA	10	Modern
M3/30 cm	KIA	30	440–340
M2/27.5 cm	KIA	27.5	490–350
M9/32 cm	KIA	32	510–370
M5/15 cm	KIA	15	530–480
RKS3/351 cm	KIA	351	710–670
M5/57.5 cm	KIA	57	870–730
M6/57.5 cm	KIA	57.5	890–750
CS/30 cm	UtC-8724	30	490–350
CS/90 cm	UtC-8725	90	970–930
CS/135	UtC-8737	135	5913–5888
BA40	UtC-8722	40	Modern
BA240	UtC-8723	240	1818–1713
BA540	UtC-8724	540	2119–1994
FC30	UtC-8719	30	Modern
FC120	UtC-8720	120	1260–1196
FC179	UtC-8721	179	1349–1297
TAP	KIA21248	35	Modern
TAP	KIA21247	85	Modern
TAP	KIA21972	115	6814–6726
TAP	KIA19405	185	6520–6460
TAP	KIA21973	290	7413–7327
TAP	KIA19406	385	11,771–11,393
APL1	KIA21274	40	445–339
APL2	Erl-9452	27	400–76
AB1	KIA21275	230	890–786
AB2	KIA27245	125	705–615
SC1	KIA21277	600	7567–7509
SC2	KIA27244	290	6780–6658
SC3	Erl-9451	95	1168–1044

4. Wetland dynamic during the Holocene

As described previously, Marajó Island and Macapá town present a regional low water salinity produced by the larger freshwater discharge from the Amazonas river as compared to the rivers from southeastern Pará and northwestern Amapá littoral (Kjerfve et al., 2002). This produced a fluvial sector and a marine-influenced littoral (Fig. 1).

The marine littoral is mainly dominated by mangrove and herbaceous flats, typical of brackish waters, while the fluvial littoral is mainly characterized by *várzea* and herbaceous vegetation, typical of freshwaters. The relationship between mangrove and sediment geochemistry has been widely investigated (Hesse, 1961; Baltzer, 1975; Lacerda et al., 1995; Alongi et al., 2000). Wetlands from northern Brazil follow well-known patterns in which salinity excludes certain species (Snedaker, 1978), leading to characteristic patterns of species zonation (Menezes et al., 2003) where the mangroves are more tolerant to soil salinity than the *várzea* forest (Gonçalves-Alvim et al., 2001; Cohen et al., 2008), and, considering the Amazon River, the salinity is basically controlled by position along the estuarine gradient (Lara and Cohen, 2006).

4.1. Marine littoral

The intertidal area of the marine littoral presents 3090 km^2 of mangroves and 90 km^2 of herbaceous flats (Cohen et al., 2009). These wetlands have occurred continually over tidal mud flats along the marine littoral of the Pará State during the Holocene and with deposition of marine organic matter during at least the Late Holocene along the marine littoral of the Amapá State (Fig. 1) (Cohen et al., 2005b, 2009; Vedel et al., 2006; Guimarães et al., 2012). During the Early Holocene, the mangrove establishment was marked by dominance of *Avicennia* trees in the Bragança littoral, while the *Rhizophora* expanded relative to *Avicennia* during the Middle and Late Holocene (Vedel et al., 2006). The pollen records indicate that mangrove areas on the Bragança Peninsula have been mainly controlled by the relative sea level during the Holocene (Cohen et al., 2005a,b), and the mangroves have migrated to higher elevated zones during the last decades, suggesting a relative sea-level rise (Cohen and Lara, 2003; Cohen et al., 2005b).

Regarding the consequences of rainfall changes during the Holocene on the marine littoral, it should have caused changes in tidal water salinity with consequences for the mangrove structure, since the mangrove vegetation height presents an inverse relationship with substrate salinity (Lara and Cohen, 2006). In addition, the upper mud flats with porewater salinity between 90 and 50‰ consist mainly of *Avicennia* and sectors with porewater salinity around 36‰ are dominated by *Rhizophora* (Cohen and Lara, 2003).

Considering the eastern Venezuela, *in situ* mangrove community was established at 6960 ± 70 year old (7936–7674 cal yr BP) (Rull et al., 1999). In the early Holocene, mangroves were dominated by *Avicennia* or co-dominated by it and *Rhizophora*. Since then, a relative sea level rise of about 13.2 cm/100 year has been the most important natural disturbance suffered by the mangrove community in Venezuela (Vilarrúbia and Rull, 2002). According to Van der Hammen (1988), during the Early Holocene the rise in sea-level in the nearby coasts of Guyana caused the replacement of savannah by mangrove vegetation, and *Avicennia* was the first mangrove-forming tree to become established.

4.2. Fluvial littoral

Pollen and isotopic data from fluvial littoral indicate that marine influence and mangrove vegetation was wider than today on Marajó Island (Smith et al., 2011) and the Macapá littoral (Guimarães et al., 2012) between >8990–8690 and 2300–2230 and >5560–5470 and 5290–5150 cal yr BP, respectively. In addition, recent isotopic and pollen data from Marajó Island confirm this marine influence and the presence of a tidal mud flat colonized by mangroves between >7520–7430 cal yr BP and ~3200 cal yr BP in the central area of this island (França et al., in press). During the last 2300–2230 cal yr BP the freshwater vegetation expanded on the Marajó Island (Smith et al., 2012), and the mangroves were isolated in a limited area (100–700 m width) along the northeastern coastal plain of Marajó Island during the Late Holocene (França et al., in press). Similarly, the freshwater vegetation expanded along the littoral of Macapá, on the edge of Amazon River, during the Late Holocene (Guimarães et al., 2012). Therefore, the data indicate higher marine influence near the mouth of Amazon River during the Early and Middle Holocene. The temporal transition between the marine to fluvial littoral produced significant geomorphologic changes, such as the replacement of old lagoons by lakes (Miranda et al., 2009; Smith et al., 2011). The different chronology between Macapá and the Marajó Island coastline, showing the transition from brackish to freshwater vegetation may be justified by the position of sampling sites along the estuarine gradient. The littoral of Macapá, where mangroves have occurred up to 5290–5150 cal yr BP, is on the edge of the Amazon River, while Lake Arari in Marajó Island, where the mangroves resisted until 2300–2230 cal yr BP, is positioned at the mouth of the Amazon (Fig. 1).

5. Controlling factors of the wetland dynamic

Deciphering the main factor responsible for the mangrove dynamic recorded in the Holocene at the mouth of the Amazon River is not straightforward. This is stated particularly considering that the region might have been undergone to the complex interaction of several factors, mostly consisting of changes in sea level, subsidence rates, and climate, the latter with potential to have affected the Amazon River discharge. The most likely is that all these factors acted together and controlled the distribution of mangrove in this region over the Holocene.

The contraction of the mangrove area during the Late Holocene at the mouth of the Amazon River could be a natural response to the progradation of coastline, following the stabilization and accumulation of mud to new mangrove colonization. However, it is notable that this process should necessarily have occurred throughout the Macapá and Marajó coastline, but rather than mangroves, freshwater vegetation (*várzea*) was established (Cohen et al., 2008; Smith et al., 2011; Guimarães et al., 2012).

The mangroves along the southeastern Pará and northwestern Amapá littoral (marine littoral) occurred continually during the Holocene and at least the Late Holocene, respectively. The greater tidal water salinity during the Early and Middle Holocene in the fluvial sector could be attributed to the episode of Atlantic sea-level rise recorded in other parts of South America (e.g., Suguio et al., 1985; Tomazelli, 1990; Rull et al., 1999; Hesp et al., 2007; Angulo et al., 2006, 2008) (Fig. 2). This event could also have produced a marine incursion along the Pará and Amapá littoral, where the relative sea-level-RSL stabilized at its current level between 7000 and 5000 yr BP (e.g., Behling and Costa, 2001; Behling et al., 2001; Behling, 2002, 2011; Cohen et al., 2005a; Souza Filho et al., 2006; Vedel et al., 2006). A transgressive phase occurred on Marajó Island in the Early to Middle Holocene. Subsequently, there was a return to the more continental conditions that prevail today in the study area (Rossetti et al., 2008). This history of RSL fluctuations on Marajó Island seems to have been affected by tectonic activity during the Late Pleistocene and Holocene. Hence, transgression was favoured during increased subsidence, when space was created to accommodate new sediments. Tectonic stability seems to have prevailed during the Middle to Late Holocene, leading to coastal progradation that culminated with more continental conditions prevailing on the island, and with the detachment of Marajó Island from mainland. It contributed to the change in coastal morphology from an estuarine dominated one into a rectilinear coast. In this process, areas with marine influence located circa 45 km inland in this island became freshwater dominated during the Late Holocene (Rossetti et al., 2008, 2012).

Hence, the post-glacial sea-level rise, combined with tectonic subsidence, caused a marine transgression. The tidal water salinity should have further increased due to low river discharge resulting from increased aridity during the Early and Middle Holocene. If river systems are considered to be integrators of rainfall over large areas (Amarasekera et al., 1997), variations in the discharge of the Amazon River during the Holocene may be a consequence of changes in rainfall rates, as recorded in many different regions of the Amazon Basin (e.g., Bush and Colinvaux, 1988; Absy et al., 1991; Sifeddine et al., 1994; Desjardins et al., 1996; Gouveia et al., 1997; Pessenda et al., 1998a,b, 2001; Behling and Hooghiemstra, 2000; Freitas et al., 2001; Sifeddine et al., 2001; Weng et al., 2002; Bush et al., 2007; Guimarães et al., 2012) (Fig. 2).

For example, the climatic conditions in the tropical Andes were significantly drier than today between 9200 and 4400 cal yr BP (Seltzer et al., 1995; Thompson et al., 1995, 2000; Moy et al., 2002; Paduano et al., 2003; Niemann and Behling, 2008). Baker et al. (2001) demonstrated that the maximum aridity and lowest level of Lake Titicaca occurred from 8000 to 5500 cal yr BP. In the eastern Bolivian Andes, a replacement of cloud forest by open, grass-dominated ecosystems occurred between ~11,500 cal yr BP and ~4500 cal yr BP (Mourguiart and Ledru, 2003). Palaeoecological records from lakes in the Peruvian Amazon indicate a dry event from 7200 cal yr BP to 3300 cal yr BP (Bush et al., 2007). In lowland Amazonian Ecuador, periods of severe drought caused significant tree mortality between 8700 and 5800 cal yr BP, and after 5800 cal yr BP more uniform conditions allowed the development of mature forests (Weng et al., 2002). In the Colombian Amazon, drier Early Holocene and wetter Late Holocene conditions have also been reported (Behling and Hooghiemstra, 2000). Concomitantly, the drier period caused the replacement of forest by open savannah in the Amazon region, which in turn gave way to forest again when precipitation increased in the Late Holocene (Bush and Colinvaux, 1988; Absy et al., 1991; Desjardins et al., 1996; Pessenda et al., 1998a,b; Freitas et al., 2001; Sifeddine et al., 2001; Behling, 2011). This trend is similar to other documented forest-savannah vegetation changes in the Amazon basin during the Early and Middle Holocene (Sifeddine et al., 1994; Gouveia et al., 1997; Pessenda et al., 1998a,b; Behling and Costa, 2000).

On the Maranhão littoral in the eastern Amazon region, isotopic analyses of soil organic matter collected in forested and woody savannah areas indicate that from approximately 10,000 and 9000 cal yr BP to 4000 cal yr BP a woody savannah expanded, probably reflecting a drier climate (Pessenda et al., 2004). From 4000–3000 cal yr BP to the present, there was a moderate and progressive increase in arboreal vegetation in the southern Amazon basin, due to the return to more humid climate conditions that were probably similar to the present day (Freitas et al., 2001; Pessenda et al., 2004). Other isotopic studies in the southern Amazon region and on a 1600 km transect covering three states of the northeastern region, ~3000 km away from the study site, indicate a drier climate during the Middle Holocene, while the data reflect forest expansion associated with a wetter period for the last 3000 years (Pessenda et al., 1998a,b).

These climatic fluctuations in the Amazonian hydrographical region control the volume of the Amazon River's inflow (Haberle and Maslin, 1999; Harris and Mix, 1999). Consequently, during the Early and Middle Holocene the Amazon River's inflow was severely reduced (Maslin and Burns, 2000; Maslin et al., 2000). Irion et al. (2009) suggest that during the dry period, the sea level rise caused a backwater effect which reached far upstream, with the silting up of the Amazon valley and the inflow of the tributaries. This allowed the development of the Amazon River floodplain in its modern setting around ~5800 cal yr BP, when the sea level reached its present level. Afterwards, with the return of a more humid climate in the region, the greater discharge of the Amazon River promoted the progressive reduction of water salinity. At present, the littoral of Macapá and Marajó Island is flooded by tidal freshwater (Santos et al., 2008; Vinzon et al., 2008; Rosario et al., 2009) that favours the development of freshwater vegetation (Cohen et al., 2008).

The modern mangrove vegetation on the fluvial sector occurs in narrow zones fed by brackish waters carried from the southeastern Pará coastline by the northern Brazil current (Fig. 1). This water influx produces a relatively higher tidal water salinity, and is probably the cause for the permanence of mangroves in the fluvial littoral, for example, in a narrow zone on the northeastern part of the Marajó Island (Behling et al., 2004; França et al., in press), where tidal water salinity is close to ~6‰ (Santos et al., 2008).

6. Conclusions

Pollen, C/N ratios, δ^{13}C and δ^{15}N data obtained from 34 sediment cores and with a time control of 72 radiocarbon dates allowed the authors to identify the establishment of a continuous marine influenced littoral along northern Brazil during the Early and Middle Holocene as a consequence of the post-glacial sea-level rise that was favoured by tectonic subsidence. The tidal water salinity should have increased due to low river discharge resulting from increased aridity during the Early and Middle Holocene. However, during the Late Holocene, the littoral near the Amazon River underwent a significant increase in fluvial influence that fragmented this mangrove belt. As a consequence, the mangrove was replaced by *várzea* vegetation, and the marine organic matter in the sediment changed to freshwater organic matter. Likely, it was caused by the increase of river freshwater discharge during the Late Holocene, which caused a significant decrease of tidal water salinity in Marajó Island and part of the Amapá coastline (Macapá). In Marajó Island, the coast morphology evolved from an estuarine dominated into a rectilinear coast due to coastal progradation. Most likely these changes in the Amazon discharge were caused by dry and wet periods recorded in the Amazonia region during the Holocene.

Acknowledgements

We thank members of the Laboratory of Costal Dynamic (LADIC-UFPA) and Center for Nuclear Energy in Agriculture (CENA-USP) and students from the Laboratory of Chemical-Oceanography for their support. This study was financed by CNPq (Project 562398/2008-2), FAPESPA (Project 104/2008), and FAPESP (Project 03615-5/2007).

References

Absy, M.L., Cleef, A., Fournier, M., Martin, L., Servant, M., Sifeddine, A., Ferreira da Silva, M., Soubies, F., Suguio, K., Turcq, B., Van Der Hammen, T.H., 1991. Mise en evidence de quatre phases d'overture de la forêt dense dans le sud-est de l'Amazonie au cours des 60,000 dernieres annees. Premiere comparison avec d'autres regions tropicales. Comptes Rendus de l'Académie des Sciences, Paris 312, 673–678 (Serie II).
Alongi, D.M., Tirendi, F., Clough, B.F., 2000. Below-ground decomposition of organic matter in forests of the mangrove *Rhizophora stylosa* and *Avicennia marina* along the arid coast of Western Australia. Aquatic Botany 68, 97–122.
Amarasekera, K.N., Lee, R.F., Williams, E.R., Eltahir, E.A.B., 1997. ENSO and the natural variability in the flow of tropical rivers. Journal of Hydrology 200, 24–39.
ANA, 2003. Hydrological Information System. On line dataset, 14.3 MB. Brazilian National Water Agency. http://hidroweb.ana.gov.br/baixar/mapa/Bacia1.zip.
Angulo, R.J., Lessa, G.C., Souza, M.C., 2006. A critical review of the mid- to late Holocene sea-level fluctuations on the eastern Brazilian coastline. Quaternary Science Reviews 25, 486–506.
Angulo, R.J., de Souza, M.C., Assine, M.L., Pessenda, L.C.R., Disaró, S.T., 2008. Chronostratigraphy and radiocarbon age inversion in the Holocene regressive barrier of Paraná, southern Brazil. Marine Geology 252, 111–119.
Baker, P.A., Seltzer, G.O., Fritz, S.C., Dunbar, R.B., Grove, M.J., Tapia, P.M., Cross, S.L., Rowe, H.D., Broda, J.P., 2001. The history of South American tropical precipitation for the past 25,000 years. Science 291, 640–643.
Baltzer, F., 1975. Solution of silica and formation of quartz and smectite in mangrove swamps and adjacent hypersaline marsh environments. In: Proceedings of the International Symposium on Biology and Management of Mangroves. Univ. Florida, pp. 482–498.
Beardsley, R.C., Candela, J., Limeburner, R., Geyer, W.R., Lentz, S.J., Castro, B.M., Cacchione, D., Carneiro, N., 1995. The M2 tide on the Amazon shelf. Journal of Geophysical Research 100, 2283–2319.
Behling, H., 1996. First report on new evidence for the occurrence of Podocarpus and possible human presence at the mouth of the Amazon during the Late-glacial. Vegetation History and Archaeobotany 5, 241–246.
Behling, H., 2001. Late Quaternary environmental changes in the Lagoa da Curuca region (eastern Amazonia) and evidence of *Podocarpus* in the Amazon lowland. Vegetation History and Archaeobotany 10, 175–183.
Behling, H., 2002. Impact of the Holocene sea-level changes in coastal, eastern and central Amazonia. Amazoniana 17, 41–52.
Behling, H., 2011. Holocene environmental dynamics in coastal, eastern and central Amazonia and the role of the Atlantic sea-level change. Geographica Helvetica 3, 208–216.
Behling, H., Costa, M.L., 2000. Holocene environmental changes from the Rio Curuá record in the Caxiuanã region, eastern Amazon Basin. Quaternary Research 53, 369–377.
Behling, H., Costa, M.L., 2001. Holocene vegetation and coastal environmental changes from Lago Crispim in northeastern Pará State, northern Brazil. Palaeogeography, Palaeoclimatology, Palaeoecology 114, 145–155.
Behling, H., Hooghiemstra, H., 2000. Holocene Amazon rainforest–savanna dynamics and climatic implications: high-resolution pollen record from Laguna Loma Linda in eastern Colombia. Journal of Quaternary Science 15, 687–695.
Behling, H., Cohen, M.C.L., Lara, R.J., 2001. Studies on Holocene mangrove ecosystem dynamics of the Bragança Peninsula in north-eastern Pará, Brazil. Palaeogeography, Palaeoclimatology, Palaeoecology 167, 225–242.
Behling, H., Cohen, M.C.L., Lara, R.J., 2004. Late Holocene mangrove dynamics of the Marajó Island in northern Brazil. Vegetation History and Archaeobotany 13, 73–80.
Bush, M.B., Colinvaux, P.A., 1988. A 7000-year pollen record from the Amazon lowlands, Ecuador. Vegetatio 76, 141–154.
Bush, M.B., Silman, M.R., Listopad, C.M.C.S., 2007. A regional study of Holocene climate change and human occupation in Peruvian Amazonia. Journal of Biogeography 34, 1342–1356.
Cohen, M.C.L., Lara, R.J., 2003. Temporal changes of mangrove vegetation boundaries in Amazonia: application of GIS and remote sensing techniques. Wetlands Ecology and Management 11, 223–231.
Cohen, M.C.L., Lara, R.J., Ramos, J.F.F., Dittmar, T., 1999. Factors influencing the variability of magnesium, calcium and potassium in waters of a mangrove creek in Bragança, North Brazil. Mangroves and Salt Marshes 3, 9–15.
Cohen, M.C.L., Behling, H., Lara, R.J., 2005a. Amazonian mangrove dynamics during the last millennium: the relative sea-level and the little Ice Age. Review of Palaeobotany and Palynology 136, 93–108.
Cohen, M.C.L., Souza Filho, P.W., Lara, R.L., Behling, H., Angulo, R., 2005b. A model of Holocene mangrove development and relative sea-level changes on the Bragança Peninsula (northern Brazil). Wetlands Ecology and Management 13, 433–443.
Cohen, M.C.L., Lara, R.J., Smith, C.B., Angélica, R.S., Dias, B.S., Pequeno, T., 2008. Wetland dynamics of Marajó Island, northern Brazil, during the last 1000 years. Catena 76, 70–77.
Cohen, M.C.L., Lara, R.J., Smith, C.B., Matos, H.R.S., Vedel, V., 2009. Impact of sea level and climatic changes on the Amazon coastal wetlands during the late Holocene. Vegetation History and Archaeobotany 18, 425–439.
Colinvaux, P.A., De Oliveira, P.E., Patiño, J.E.M., 1999. Amazon Pollen Manual and Atlas. Hardwood Academic, Amsterdam, 332 pp.

Desjardins, T., Filho, A.C., Mariotti, A., Chauvel, A., Girardin, C., 1996. Changes of the forest savanna boundary in Brazilian Amazonia during the Holocene as revealed by soil organic carbon isotope ratios. Oecologia 108, 749–756.

Eisma, D., Augustinus, P.G.E.F., Alexander, C., 1991. Recent and subrecent changes in the dispersal of Amazon mud. Netherlands Journal of Sea Research 28, 181–192.

Faegri, K., Iversen, J., 1989. Textbook of Pollen Analysis, fourth ed. Wiley, Chichester, 328 pp.

França, M., Francisquini, M.I., Cohen, M.C.L., Pessenda, L.C.R., Rosseti, D.F., Guimarães, J., Smith, C.B. The last mangroves of Marajó Island – Eastern Amazon: impact of climate and/or relative sea-level changes. Review of Palaeobotany and Palynology, in press.

Freitas, H.A., Pessenda, L.C.R., Aravena, R., Gouveia, S.E.M., Ribeiro, A.S., Boulet, R., 2001. Late Quaternary vegetation dynamics in the southern Amazon basin inferred from carbon isotopes in soil organic matter. Quaternary Research 55, 39–46.

Gallo, M.N., Vinzon, S., 2005. Generation of over tides and compound tides in Amazon estuary. Ocean Dynamics 55, 441–448.

Gonçalves-Alvim, S.J., Vaz dos Santos, M.C.F., Fernandes, G.W., 2001. Leaf gall abundance on *Avicennia germinans* (Avicenniaceae) along an interstitial salinity gradient. Biotropica 33, 69–77.

Gouveia, S.E.M., Pessenda, L.C.R., Aravena, R., Boulet, R., Roveratti, R., Gomes, B.M., 1997. Dinâmica de vegetações durante o Quaternário recente no sul do Amazonas indicada pelos isótopos do carbono (12C, 13C e 14C). Geochimica Brasiliensis 11, 355–367.

Guimarães, J.T.F., Cohen, M.C.L., Pessenda, L.C.R., França, M.C., Smith, C.B., Nogueira, A.C.R., 2012. Mid- and late-Holocene sedimentary process and palaeovegetation changes near the mouth of the Amazon River. The Holocene 22, 359–370.

Haberle, S.G., Maslin, M.A., 1999. Late Quaternary vegetation and climate change in the Amazon basin based on a 50,000 year pollen record from the Amazon fan, ODP site 932. Quaternary Research 51, 27–38.

Harris, S.E., Mix, A.C., 1999. Pleistocene precipitation balance in the Amazon basin recorded in deep sea sediments. Quaternary Research 51, 14–26.

Hesp, P.A., Dillenburg, S.R., Barboza, E.G., Clerot, L.C.P., Tomazelli, L.J., Zouain, R.N.A., 2007. Morphology of the Itapeva to Tramandai transgressive dunefield barrier system and mid to late Holocene sea level change. Earth Surface Process and Landforms 32, 407–414.

Hesse, P.R., 1961. Some differences between the soils of *Rhizophora* and *Avicennia* mangrove swamp in Sierra Leone. Plant and Soil 14, 335–346.

Hesse, M., Halbritter, H., Zetter, R., Weber, M., Buchner, R., Frosch-Radivo, A., Ulrich, S., 2008. Pollen Terminology: an Illustrated Handbook. Springer, New York, 264 pp.

Hutchings, P., Saenger, P., 1987. Ecology of Mangroves. Queensland University Press, 338 pp.

IDESP Institute of Social and Economic development of the Pará, 1974. Integrated Studies of Marajó Island. Belém. 333 pp.

Irion, G., Müller, J., Morais, J.O., Keim, G., Nunes de Mello, J., Junk, W.J., 2009. The impact of Quaternary sea level changes on the evolution of the Amazonian lowland. Hydrological Processes 23, 3168–3172.

Junk, W.J., Piedade, M.T.F., 2004. Status of knowledge, ongoing research, and research needs in Amazonia wetlands. Wetlands Ecology and Management 12, 597–609.

Kjerfve, B., Lacerda, L.D., 1993. Mangroves of Brazil. In: Lacerda, L.D. (Ed.), Conservation and Sustainable Utilization of Mangrove Forests in Latin America and Africa Regions. Part I — Latin America. ITTO/International Society for Mangrove Ecosystems, Okinawa, Japan, pp. 245–272.

Kjerfve, B., Perillo, G.M.E., Gardner, L.R., Rine, J.M., Dias, G.T.M., Mochel, F.R., 2002. Morphodynamics of muddy environments along the Atlantic coasts of North and South America. In: Healy, T., Wang, Y., Healy, J.A. (Eds.), Muddy Coasts of the World: Processes, Deposits and Functions. Elsevier Science, Amsterdam, pp. 479–532.

Lacerda, L.D., Ittekkot, V., Patchineelam, S.R., 1995. Biogeochemistry of mangrove soil organic matter: a comparison between *Rhizophora*, *Avicennia* soils in southeastern Brazil. Estuarine, Coastal and Shelf Science 40, 713–720.

Lara, J.R., Cohen, M.C.L., 2006. Sediment porewater salinity, inundation frequency and mangrove vegetation height in Bragança, North Brazil: an ecohydrology-based empirical model. Wetlands Ecology and Management 4, 49–358.

Lara, R.J., Cohen, M.C.L., 2009. Palaeolimnological studies and ancient maps confirm secular climate fluctuations in Amazonia. Climatic Change 94, 399–408.

Latrubesse, E.M., Franzinelli, E., 2002. The Holocene alluvial plain of the middle Amazon River, Brazil. Geomorphology 44, 241–257.

Ledru, M.P., 2001. Late Holocene rainforest disturbance in French Guiana. Review of Palaeobotany and Palynology 115, 161–176.

Lentz, S.J., Limeburner, R., 1995. The Amazon River Plume during AMASSEDS: spatial characteristics and salinity variability. Journal of Geophysical Research 100, 2355–2375.

Maslin, M.A., Burns, S.J., 2000. Reconstruction of the Amazon Basin effective moisture availability over the past 14,000 years. Science 290, 2285–2287.

Maslin, M.A., Durham, E., Burns, S.J., Platzman, E., Grootes, P., Greig, S.E.J., Nadeau, M.J., Schleicher, M., Pflaumann, U., Lomax, B., Rimington, N., 2000. Palaeoreconstruction of the Amazon River freshwater and sediment discharge using sediments recovered at Site 942 on the Amazon Fan. Journal of Quaternary Science 15, 419–434.

McGinley, M., 2007. Marajó varzea. In: Cleveland, C.J. (Ed.), Encyclopedia of Earth. Environmental Information Coalition, National Council for Science and the Environment, Washington. http://www.eoearth.org/article/Marajo_varzea (accessed 25.08.12).

Menezes, M., Berger, U., Worbes, M., 2003. Annual growth rings and long-term growth patterns of mangrove trees from the Bragança peninsula, North Brazil. Wetlands Ecology and Management 1, 33–242.

Miranda, M.C.C., Rossetti, D.F., Pessenda, L.C.R., 2009. Quaternary paleoenvironments and relative sea-level changes in Marajó Island (Northern Brazil): facies, δ^{13}C, δ^{15}N and C/N. Palaeogeography, Palaeoclimatology, Palaeoecology 282, 19–31.

Monteiro, S.M., 2009. Dinâmica dos parâmetros abióticos na zona de mistura do estuario do rio Paracauarí – Ilha de Marajó (PA). Dissertação de Mestrado, Instituto de Geociências, Universidade Federal do Pará, 135p.

Mourguiart, P., Ledru, M.P., 2003. Last Glacial Maximum in an Andean cloud forest environment (Eastern Cordillera, Bolivia). Geology 31, 195–198.

Moy, C.M., Seltzer, G.O., Rodbell, D.T., Anderson, D.M., 2002. Variability of El Nino/Southern Oscillation activity at millennial timescales during the Holocene epoch. Nature 420, 162–165.

Niemann, H., Behling, H., 2008. Late Quaternary vegetation, climate and fire dynamics inferred from the El Tiro record in the southeastern Ecuadorian Andes. Journal of Quaternary Sciences 3, 203–212.

Paduano, G.M., Bush, M.B., Baker, P.A., Fritz, S.C., Seltzer, G.O., 2003. A vegetation and fire history of Lake Titicaca since the Last Glacial Maximum. Palaeogeography, Palaeoclimatology, Palaeoecology 194, 259–279.

Pessenda, L.C.R., Gomes, B.M., Aravena, R., Ribeiro, A.S., Boulet, R., Gouveia, S.E.M., 1998a. The carbon isotope record in soils along a forest-cerrado ecosystem transect: implications for vegetation changes in the Rondonia state, southwestern Brazilian Amazon region. The Holocene 8, 631–635.

Pessenda, L.C.R., Gouveia, S.E.M., Aravena, R., Gomes, B.M., Boulet, R., Ribeiro, A.S., 1998b. ^{14}C dating and stable carbon isotopes of soil organic matter in forest savanna boundary areas in the southern Brazilian Amazon region. Radiocarbon 40, 1013–1022.

Pessenda, L.C.R., Boulet, R., Aravena, R., Rosolen, V., Gouveia, S.E.M., Ribeiro, A.S., Lamotte, M., 2001. Origin and dynamics of soil organic matter and vegetation changes during the Holocene in a forest-savanna transition zone, Brazilian Amazon region. The Holocene 11, 250–254.

Pessenda, L.C.R., Ribeiro, A.S., Gouveia, S.E.M., Aravena, R., Boulet, R., Bendassoli, J.A., 2004. Vegetation dynamics during the late Pleistocene in the Barreirinhas region, Maranhão State, northeastern Brazil, based on carbon isotopes in soil organic matter. Quaternary Research 62, 183–193.

Pugh, D.T., 1987. Tides, Surges and Mean Sea-level: a Handbook for Engineers and Scientists. Wiley, London, 486 pp.

Reimer, P.J., Baillie, M.G.L., Bard, E., Bayliss, A., Beck, J.W., Blackwell, P.G., Bronk Ramsey, C., Buck, C.E., Burr, G.S., Edwards, R.L., Friedrich, M., Grootes, P.M., Guilderson, T.P., Hajdas, I., Heaton, T.J., Hogg, A.G., Hughen, K.A., Kaiser, K.F., Kromer, B., Mccormac, F.G., Manning, S.W., Reimer, R.W., Richards, D.A., Southon, J.R., Talamo, S., Turney, C.S.M., Van der Plicht, J., Weyhenmeyer, C.E., 2009. IntCal09 and Marine09 radiocarbon age calibration curves, 0–50,000 years cal BP. Radiocarbon 51 (4), 1111–1150. New Haven.

Rosario, R.P., Bezerra, M.O.M., Vinzon, S.B., 2009. Dynamics of the saline front in the Northern Channel of the Amazon River – influence of fluvial flow and tidal range (Brazil). Journal of Coastal Research 2, 503–514.

Rossetti, D.F., Valeriano, M.M., Goes, A.M., Thales, M., 2008. Palaeodrainage on Marajó Island, northern Brazil, in relation to Holocene relative sea-level dynamics. The Holocene 18, 01–12.

Rossetti, D.F., Souza, L.S.B., Prado, R., Elis, V.R., 2012. Neotectonics in the northern equatorial Brazilian margin. Journal of South American Earth Sciences 37, 175–190.

Roubik, D.W., Moreno, J.E., 1991. Pollen and Spores of Barro Colorado Island, vol. 36. Missouri Botanical Garden, St. Louis, 268 pp.

Rull, V., Vegas-Vilarrùbia, T., Espinoza, N.P., 1999. Palinological record in an early-mid Holocene mangrove in eastern Venezuela: implications for sea-level rise and disturbance history. Journal of Coastal Research 15, 496–504.

Santos, M.L.S., Medeiros, C., Muniz, K., Feitosa, F.A.N., Schwamborn, R., Macedo, S.J., 2008. Influence of the Amazon and Pará Rivers on water composition and phytoplankton biomass on the Adjacent Shelf. Journal of Coastal Research 24, 585–593.

Schaeffer-Novelli, Y., Cintrón Molero, G., Rothleder Adaime, R., Camargo, T.M.D., 1990. Variability of mangrove ecosystems along the Brazilian coast. Estuaries 13, 204–218.

Seltzer, G.O., Rodbell, D.T., Abbott, M., 1995. Andean glacial lakes and climate variability since the Last Glacial Maximum. Bulletin – Institut Francais d'Etudes Andines 24, 539–549.

Semeniuk, V., 1994. Predicting the effect of sea-level rise on mangroves in northwestern Australia. Journal of Coastal Research 10, 1050–1076.

Sifeddine, A., Bertrand, P., Fournier, M., Martin, L., Servant, M., Soubiès, F., Suguio, K., Turcq, B., 1994. La sédimentation organique lacustre en milieu tropical humide (Carajás, Amazonie orientale, Brésil): relation avec les changements climatiques au cours des 60000 dernières années. Bulletin de La Société Geologique de France 165, 613–621.

Sifeddine, A., Marint, L., Turcq, B., Volkmer-Ribeiro, C., Soubiès, F., Cordeiro, R.C., Suguio, K., 2001. Variations of the Amazonian rainforest environment: a sedimentological record covering 30,000 years. Palaeogeography, Palaeoclimatology, Palaeoecology 168, 221–235.

Smith, C.B., Cohen, M.C.L., Pessenda, L.C.R., França, M., Guimarães, J.T.F., Rossetti, D.F., 2011. Holocene coastal vegetation changes at the mouth of the Amazon River. Review of Palaeobotany and Palynology 168, 21–30.

Smith, C.B., Cohen, M.C.L., Pessenda, L.C.R., França, M.C., Guimarães, J.T.F., 2012. Holocenic proxies of sedimentary organic matter and the evolution of Lake Arari-Northern Brazil. Catena 90, 26–38.

Snedaker, S.C., 1978. Mangroves: their value and perpetuation. Natural Resources 16, 179–188.

Souza Filho, P.W.M., Cohen, M.C.L., Lara, R.J., Lessa, G.C., Koch, B., Behling, H., 2006. Holocene coastal evolution and facies model of the Bragança macrotidal flat on the Amazon mangrove coast, Northern Brazil. Journal of Coastal Research 39, 306–310.

Suguio, K., Martin, L., Bittencourt, A.C.S.P., Dominguez, J.M.L., Flexor, J.M., Azevedo, A.E.G., 1985. Flutuações do Nível do Mar durante o Quaternário Superior ao longo do Litoral Brasileiro e suas Implicações na Sedimentação Costeira. Revista Brasileira de Geociências 15, 273–286.

Thompson, L.G., Mosley-Thompson, E., Davis, M.E., Lin, P.-N., Henderson, K.A., Cole-Dai, J., Bolsan, J.F., Liu, K.G., 1995. Late glacial stage and Holocene tropical ice core records from Huascaran, Peru. Science 269, 46–50.

Thompson, L.G., Mosley-Thompson, E., Henderson, K.A., 2000. Ice core palaeoclimate records in tropical South America since the Last Glacial Maximum. Journal of Quaternary Science 15, 377–394.

Toledo, M.B., Bush, M.B., 2007. A mid-Holocene environmental change in Amazonian savannas. Journal of Biogeography 34, 1313–1326.

Toledo, M.B., Bush, M., 2008. Vegetation and hydrology changes in Eastern Amazonia inferred from pollen record. Anais da Academia Brasileira de Ciências 80, 191–203.

Tomazelli, L.J., 1990. Contribuição ao estudo dos sistemas deposicionais Holocênicos do Nordeste da Província Costeira do Rio Grande do Sul, com Ênfase no Sistema Eölico. PhD thesis, Porto Alegre, Universidade Federal do Rio Grande do Sul, 270 pp.

Van der Hammen, T., 1974. The Pleistocene changes of vegetation and climate in tropical South America. Journal of Biogeography 1, 3–26.

Van der Hammen, T., 1988. South America. In: Huntley, B., Webb III, T. (Eds.), Vegetation History. Kluwer Acad. Pub., Dordrecht, The Netherlands, pp. 307–337.

Vannucci, M., 1999. Os manguezais e nós: Uma síntese de percepcões. ESDUP, São Paulo, 233 pp.

Vedel, V., Behling, H., Cohen, M.C.L., Lara, R.J., 2006. Holocene mangrove dynamics and sea-level changes in Taperebal, northeastern Pará State, northern Brazil. Vegetation History and Archaeobotany 15, 115–123.

Vilarrúbia, T.V., Rull, V., 2002. Natural and human disturbance history of the Playa Medina mangrove community (Eastern Venezuela). Caribbean Journal of Science 38, 66–76.

Vinzon, B.S., Vilela, C.P.X., Pereira, L.C.C., 2008. Processos físicos na Plataforma Continental Amazônica. Relatório-Técnico, Potenciais Impactos Ambientais do Transporte de Petróleo e Derivados na Zona Costeira Amazônico. Petrobrás, Brasil, 31 pp.

Weng, C., Bush, M.B., Athens, J.S., 2002. Two histories of climate change and hydrarch succession in Ecuadorian Amazonia. Review of Paleobotany and Palynology 120, 73–90.

Wolanski, E., Mazda, Y., King, B., Gay, S., 1990. Dynamics, flushing and trapping in Hinchinbrook Channel, a giant mangrove swamp, Australia. Estuarine, Coastal and Shelf Science 31, 555–579.

Zarin, D.J., Pereira, V.F.G., Raffles, H., Rabelo, F.G., Pinedo-Vasquez, M., Congalton, R.G., 2001. Landscape changes in tidal floodplains near the mouth of the Amazon River. Forest Ecology and Management 154, 383–393.